POLITECNICO DI TORINO
Repository ISTITUZIONALE

A data-driven framework for predicting mechanical properties of coal–rock composites in deep mining

Original
A data-driven framework for predicting mechanical properties of coal–rock composites in deep mining / Ou, Q., Lacidogna, G., Chen, L., Hou, X., Hu, X., Song, J.. - In: ACTA GEOPHYSICA. - ISSN 1895-6572. - STAMPA. - 74:5(2026), pp. 1-17. [10.1007/s11600-026-01946-w]

Availability:
This version is available at: 11583/3015381 since: 2026-09-11T15:11:32Z

Publisher:
Springer

Published
DOI:10.1007/s11600-026-01946-w

Terms of use:

This article is made available under terms and conditions as specified in the corresponding bibliographic description in the repository

Publisher copyright

(Article begins on next page)

18 October 2026

Acta Geophysica (2026) 74:257
https://doi.org/10.1007/s11600-026-01946-w

RESEARCH ARTICLE - APPLIED GEOPHYSICS

A data-driven framework for predicting mechanical properties of coal–rock composites in deep mining

Qinghua Ou[1] · Giuseppe Lacidogna[2] · Luwang Chen[1] · Xiaowei Hou[1] · Xunjian Hu[3] · Jiawei Song[1]

Received: 29 November 2025 / Accepted: 29 June 2026
© The Author(s) 2026

Abstract

The depletion of shallow coal resources necessitates the advancement of deep mining operations, where accurate prediction of coal–rock composite mechanical behavior is critical for disaster prevention. This study systematically develops and evaluates a machine learning (ML) framework for predicting key mechanical properties. A dataset of 162 experimental results was collected, incorporating ten input features such as densities, elastic modulus, uniaxial compressive strengths (UCSs), and key ratio parameters of coal–rock components. Five base models, namely backpropagation neural network (BPNN), extreme gradient boosting (XGBoost), support vector machine (SVM), extreme learning machine (ELM), and random forest (RF), were optimized using the sparrow search algorithm (SSA). The results show that the SSA–SVM model achieved the best prediction accuracy on test data, with determination coefficients of 0.90 for composite UCS (U_{rc}) and 0.85 for elastic modulus (E_{rc}). Feature importance analysis highlighted the significant influence of coal proportion (R_c) and strength ratios (R_u) on composite mechanical performance. As R_c increases, the overall composite strength decreases. Higher strength ratios also alter load-transfer efficiency between coal and rock and increase the risk of interfacial failure. This study provides data-driven insights for designing safer underground support systems in deep mines and mitigating mining disasters.

Keywords Machine learning · Coal–rock composites · Compressive strength · Feature importance analysis

Highlights

- SSA-optimized ML models predict coal-rock composite UCS and elastic modulus well.
- SSA-SVM model achieved highest accuracy (R2=0.90 for UCS, R2=0.85 for E).
- Coal proportion and rock-to-coal strength ratio dominate composite failure mechanisms.
- Data-driven insights enable safety design for deep mining hazard mitigation.

Introduction

The declining availability of shallow coal reserves is pushing mining operations into deeper geological formations. In these challenging environments, complex stress conditions and intense extraction processes dramatically increase risks of critical hazards like rockbursts and coal–gas outbursts (He et al. 2023, 2021; Qiao et al. 2024; Wang et al. 2021). These disasters predominantly originate from structural weak points—particularly coal–rock interfaces in mine roadways and lithological transition zones near mined-out areas (Chen et al. 2022; Fu et al. 2023; Niu et al. 2022). Figure 1 illustrates typical geological configurations of coal–rock/soft–hard rock composites. Research indicates that these catastrophic events originate from instability in composite

Edited by Dr. Ahmed E. Radwan (ASSOCIATE EDITOR) / Dr. Anne Neska (CO-EDITOR-IN-CHIEF).

✉ Giuseppe Lacidogna
giuseppe.lacidogna@polito.it

1 School of Resources and Environmental Engineering, Hefei University of Technology, Hefei 230009, China

2 Department of Structural, Geotechnical and Building Engineering, Politecnico di Torino, Corso Duca degli Abruzzi 24, 10129 Turin, Italy

3 Research Center of Coastal and Urban Geotechnical Engineering, Zhejiang University, Hangzhou 310058, China

Published online: 02 September 2026

systems (Huang and Liu 2013; Lai et al. 2024; Li et al. 2021; Qiu et al. 2020). Crucially, conventional testing methods focusing on single materials prove inadequate for evaluating burst risks in composite structures, underscoring the requirement for prediction of composite mechanical properties (uniaxial compressive strength (UCS) and elastic modulus).

In recent decades, characterizing coal–rock composite strength has become crucial for geomechanical assessments. UCS and elastic modulus are typically determined by uniaxial compression tests following standards proposed by the American Society for Testing and Materials (ASTM) (2023) or the International Society for Rock Mechanics (ISRM) (Ulusay and Hudson 2007). Experimental studies have identified key factors such as coal–rock height ratio (Xie et al. 2019; Yin et al. 2023), interface inclination angle (Shen et al. 2022; Wang et al. 2020a; Xu et al. 2024a; Yu et al. 2021), interfacial strength (Gao et al. 2023; Li et al. 2015; Xu et al. 2024b), and strength differentials between coal and rock (Liu et al. 2018; Zhao et al. 2014) that control the mechanical behavior of composites. It has been reported that composite UCS and elastic modulus values scale positively with rock content (Tian et al. 2024; Wang et al. 2020b). Notably, coal properties exert greater influence than rock characteristics on composite behavior (Wang et al. 2024; Yang et al. 2020), with coal components showing higher damage levels and elastic energy release during failure (Tan et al. 2022; Zhao et al. 2024). Acoustic emission (AE) monitoring has emerged as a vital tool in geomechanical investigations (Jiang et al. 2024a, 2024b; Wang et al. 2025; Zhu et al. 2024), particularly for characterizing failure mechanisms and potential precursors of coal–rock composites (Jing et al. 2025, 2023, 2024).

However, practical experimental constraints arise from the brittle nature of coal specimens that complicate preparation processes, coupled with insufficient sample quantities that limit statistical reliability (Hu et al. 2023; Zhang et al. 2022). Existing theoretical models developed for homogeneous materials prove inadequate for composites due to unresolved interactions between material strengths, composition ratios, and interfacial geometries (Hoek and Brown 2019; Huang et al. 2022; Shaunik and Singh 2019). Furthermore, knowledge gaps remain regarding how multiple measurable parameters are jointly associated with the mechanical behavior of coal–rock composites. Data-driven models, combined with feature importance and correlation analyses, may provide preliminary insights into these coupled effects.

Machine learning (ML) has become a powerful tool for addressing complex nonlinear problems in engineering geology (Fathipour-Azar 2021; Jitchaijaroen et al. 2024; Kakasor Ismael Jaf et al. 2023; Paudel et al. 2023; Rajabi et al. 2021; Tran et al. 2024; Xu et al. 2023). Although ML models excel at identifying intricate parameter relationships, they typically lack interpretability regarding directional dependencies between input variables and mechanical responses. Successful application requires careful integration of geological expertise with optimized data processing, model selection, and validation strategies (Indraratna et al. 2023; Kumar et al. 2024). Numerous algorithms demonstrate strong predictive capabilities for UCS and elastic modulus, ranging from artificial neural networks (ANNs) (Dehghan et al. 2010; Yilmaz and Yuksek 2009) and support vector machines (SVM) (Ceryan 2014) to ensemble methods like random forest (RF) (Barzegar et al. 2019) and extreme gradient boosting (XGBoost) (Jodeiri Shokri et al. 2024). Recent advancements combine these models with bio-inspired optimization algorithms such as sparrow search algorithm (SSA) (Wang et al. 2023a), gray wolf optimizer (GWO) (Li et al. 2023), and particle swarm optimization (PSO) (Ngo et al. 2023), which significantly enhances computational efficiency and prediction accuracy. Studies like Khatti and Grover (2024) demonstrate systematic approaches for optimizing input variables (including density, wave velocity, and elastic modulus) across eight ML models to maximize UCS prediction performance. Emerging techniques integrating nondestructive testing (ultrasonic pulse velocity, rebound hammer) with ML predictions show strong correlations with conventional destructive tests (Aboutaleb et al. 2017; Han et al. 2019; Wang et al. 2023b). However, current research predominantly focuses on homogeneous rock types (e.g., sandstones, limestones), leaving critical knowledge gaps in understanding the failure mechanisms and parameter interactions specific to coal–rock composites. The mechanical interdependencies between coal and rock components in these heterogeneous systems remain poorly quantified, particularly regarding how material properties, interface geometries, and loading conditions jointly influence failure processes. This underscores the need for targeted investigations combining advanced ML techniques with dedicated composite mechanics studies.

This study develops, validates, and interprets a machine learning framework for predicting the UCS and elastic modulus of coal–rock composites using five SSA-optimized models: backpropagation neural network (BPNN), extreme gradient boosting (XGBoost), support vector machine (SVM), extreme learning machine (ELM), and random forest (RF). The main contributions of this study are fourfold: (1) A comprehensive dataset containing 162 coal–rock composite samples with different lithological combinations was compiled and analyzed; (2) based on this dataset, five models were trained and utilized for prediction, validating the rationality of employing ML methods to predict parameters of coal–rock composite samples; (3) a comprehensive analysis of feature importance was conducted to interpret the underlying principles of the data-driven findings; (4) an in-depth discussion on the limitations of the models and their potential for practical application in deep mining engineering was provided.

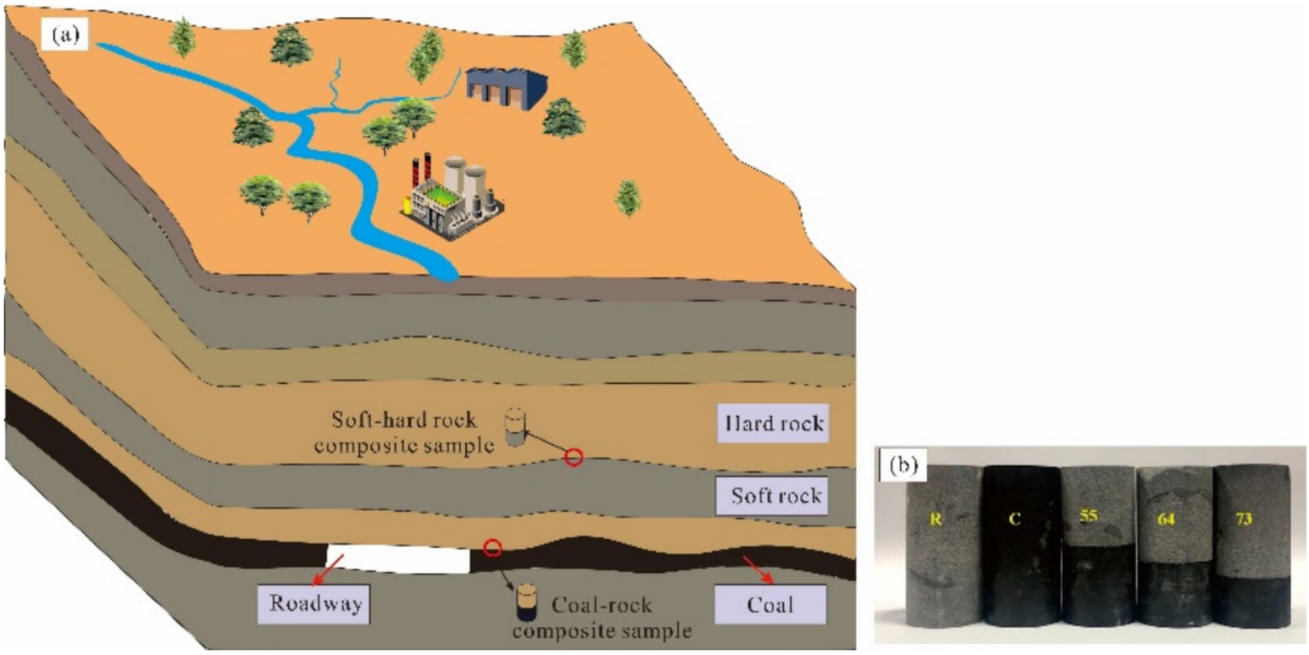

Fig. 1 Coal–rock composite and soft–hard rock composite: (a) in situ schematic diagram, (b) composite samples (Guo et al. 2023)

Dataset and preprocessing

Data sources and preprocessing

A comprehensive dataset of 162 coal–rock composite specimens was compiled from 47 published experimental studies (full references in Online Appendix A). To improve data consistency and quality, several preprocessing procedures were implemented before model development. All variables were converted to consistent SI units, and only specimens with comparable cylindrical dimensions (nominally 50 mm in diameter and 100 mm in height) were retained. Boxplot analysis was further used to detect potential outliers, and extreme values were checked against the original publications; those associated with clear reporting errors were excluded. In addition, for studies reporting multiple specimens under identical conditions, mean values were calculated to reduce within-study variability.

The source studies generally followed ISRM or ASTM procedures. Most tests used standard cylindrical specimens, servo-controlled uniaxial loading, continuous load–displacement recording, peak stress as the maximum sustained load, and elastic modulus derived from the linear segment of the stress–strain curve.

However, some variations in loading rate, end conditions, and data acquisition procedures may still exist across different laboratories. These differences may introduce additional uncertainty into the compiled dataset and should be recognized as an inherent limitation of multi-source data aggregation.

Variable selection and description

A total of ten variables were considered, including densities (D_r for rock and D_c for coal), elastic moduli (E_r for rock and E_c for coal), uniaxial compressive strengths (U_r for rock and U_c for coal), the rock-to-coal property ratios (R_d for density, R_E for elastic modulus, and R_u for UCS), and coal proportion (R_c). The composite uniaxial compressive strength (U_{rc}) and composite elastic modulus (E_{rc}) were defined as the target outputs.

The ten input variables were selected to balance physical interpretability, engineering measurability, and data availability (Dehghan et al. 2010; Hu et al. 2023). They cover three complementary aspects of coal–rock composite behavior: intrinsic properties of the constituent materials, relative property mismatch between rock and coal, and the structural proportion of the weaker coal phase. Therefore, these variables provide a compact but physically meaningful representation of both absolute material effects and coal–rock compatibility for the present dataset. The selected variables should not be interpreted as a statistically optimal feature subset; rather, they represent a practically measurable and mechanically interpretable input set suitable for the current data-driven framework.

Statistical analysis and feature selection

The statistical characteristics of the selected variables are summarized in Table 1, with the full dataset provided in Online Appendix A. The data cover a relatively broad range of underground mining conditions. For example, rock UCS ranges from 20 to 141 MPa, whereas coal UCS ranges from 5 to 44 MPa. The distributions of the input variables are further illustrated by violin plots in Fig. 2, which combine quartile ranges, median values, and kernel density estimation to visualize data variability.

The dataset exhibits several notable outliers, particularly in elastic modulus measurements, which may pose

Table 1 Statistical indicators of variables

variables	Mean	Standard deviation	Min	25%	50%	75%	Max
Rock density (D_r, kg/m^3)	2485.09	148.09	2130.00	2400.00	2500.00	2580.00	2800.00
Coal density (D_c, kg/m^3)	1342.39	59.34	1229.00	1300.00	1340.00	1383.00	1473.60
Elastic modulus of rock (E_r, GPa)	8.64	7.00	2.03	4.79	6.71	9.17	32.97
Elastic modulus of coal (E_c, GPa)	1.80	0.88	0.48	1.31	1.61	2.32	6.72
UCS of rock (U_r, MPa)	66.26	33.08	20.31	36.37	58.49	87.30	141.29
UCS of coal (U_c, MPa)	17.99	8.43	4.87	12.47	15.50	24.97	43.70
Density ratio of rock to coal (R_d)	1.85	0.11	1.31	1.78	1.85	1.92	2.16
Elastic modulus ratio of rock to coal (R_e)	5.13	3.39	0.85	2.81	3.86	7.79	20.33
UCS ratio of rock to coal (R_u)	4.51	3.03	0.72	2.18	3.84	5.98	17.39
Coal proportion (R_c)	0.43	0.16	0.05	0.30	0.50	0.50	0.88
Composite UCS (U_{rc}, MPa)	23.47	10.24	5.61	15.94	21.20	28.25	62.09
Composite elastic modulus (E_{rc}, GPa)	3.02	2.03	0.54	1.80	2.61	3.40	15.19

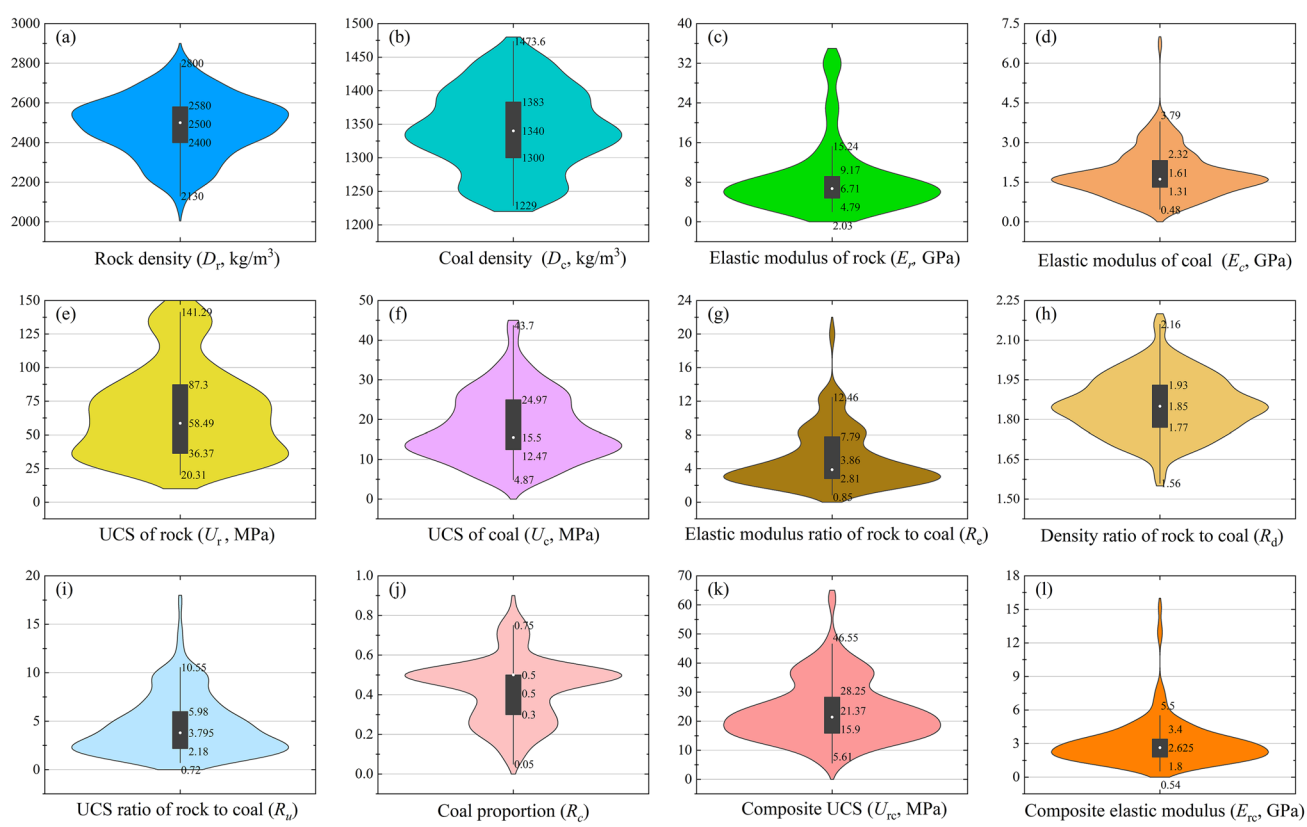

Fig. 2 Violin plots of input and output variables

challenges for model fitting during training and validation. To further investigate variables interdependence and support feature interpretation, pairwise correlation analysis was performed, as shown in Fig. 3. Spearman's rank correlation coefficient was adopted instead of Pearson's correlation coefficient because of its greater robustness to outliers and potential nonlinearity in the data. Although no strict feature elimination was performed, the distribution and correlation analyses support the relevance of the selected variables.

The results indicate that the composite strength (U_{rc}) and composite elastic modulus (E_{rc}) are positively correlated with the corresponding mechanical properties of the coal and rock components, which is generally consistent with engineering expectations. In contrast, U_{rc} shows a negative correlation with coal proportion (R_c) and the rock-to-coal strength ratio (R_u), suggesting that a stronger contrast between rock and coal properties may reduce the integrity of the composite system. Compared with the direct mechanical parameters such as UCS and elastic modulus, R_c shows weaker associations with some intrinsic material variables, indicating that it should be interpreted mainly as a structural proportion parameter rather than an intrinsic material property.

Data partitioning and normalization

Following common practice in regression modeling, the dataset was randomly divided into training and testing subsets at a ratio of 80:20 (Qiu et al. 2023). This resulted in 130 training samples and 32 testing samples, providing sufficient data for model development while preserving an independent dataset for performance evaluation.

Before model training, all input features were normalized to the [0, 1] range using min–max scaling to eliminate scale disparities among variables and improve optimization efficiency. The normalization was performed as follows:

$$X_i = \frac{X - X_{min}}{X_{max} - X_{min}} \tag{1}$$

where X_i is the normalized value; $X_{\min}$ and $X_{\max}$ are minimum and maximum values of the corresponding feature, respectively.

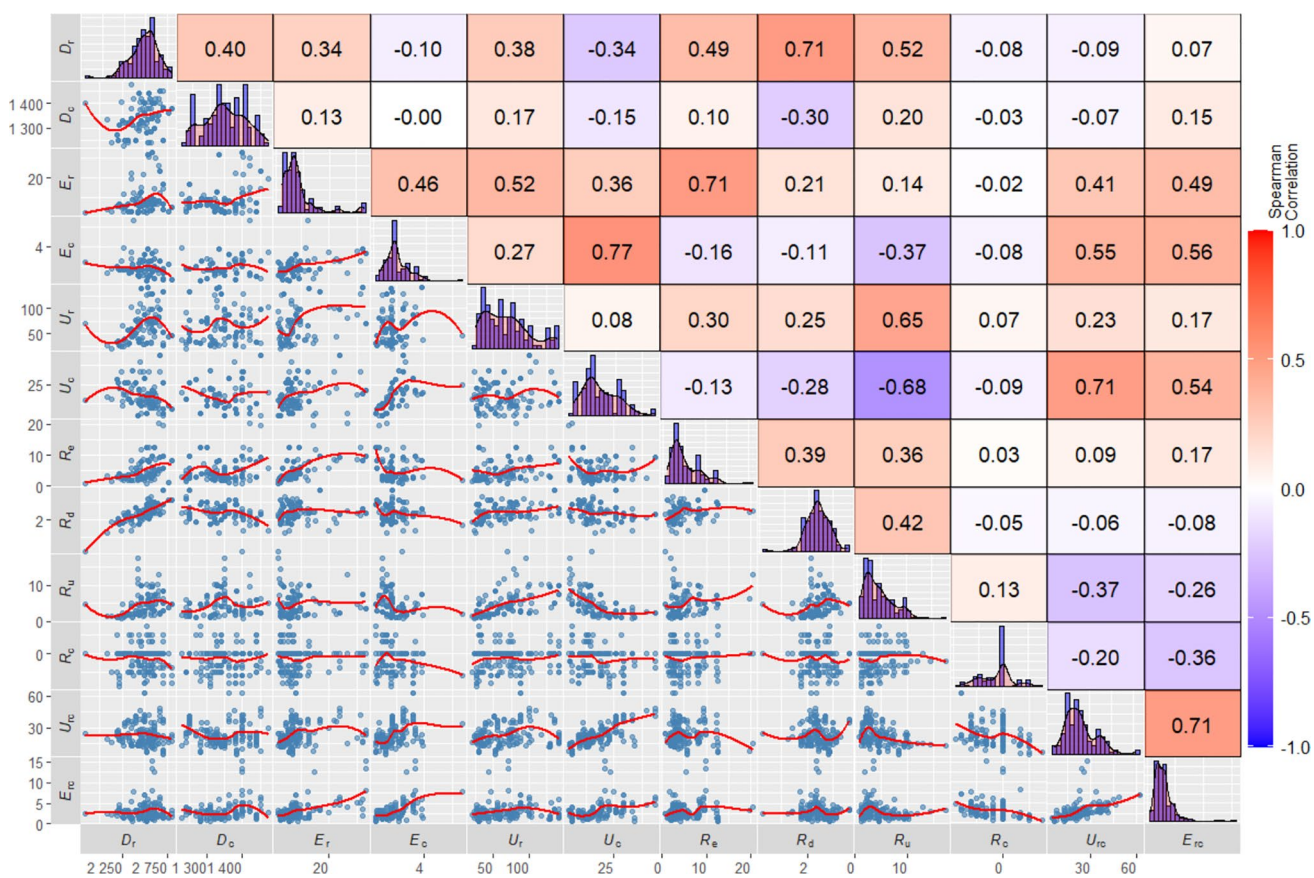

Fig. 3 Spearman correlation matrix of the input and output variables

ML methodology

Overview of ML algorithms

Five representative machine learning models, namely BPNN (Rumelhart et al. 1986), XGBoost (Chen and Guestrin 2016), SVM (Drucker et al. 1996), ELM (Huang et al. 2006), and RF (Breiman 2001), were employed in this study to predict the uniaxial compressive strength and elastic modulus of coal–rock composites. These models were selected because they represent three commonly used nonlinear regression paradigms, namely neural-network-based, kernel-based, and tree-based learning, and thus provide a broad basis for comparing predictive behavior under the same dataset and evaluation framework.

BPNN and ELM were included as representative neural-network models because of their ability to approximate nonlinear input–output relationships, although their performance may be sensitive to network structure or initialization. SVM was adopted as a representative kernel-based model because of its strong generalization ability, especially for relatively limited datasets. XGBoost and RF were selected as representative tree-based ensemble models because of their robustness in handling nonlinear relationships and feature interactions.

To ensure a fair comparison, all five models were trained using the same input variables, target outputs, data partition, and evaluation metrics. Their key hyperparameters were optimized using SSA so that the comparison reflected differences in model characteristics rather than arbitrary parameter selection. Detailed implementation and optimization procedures are described in Sects. "Sparrow search algorithm for optimization" and "Model implementation and evaluation metrics."

Sparrow search algorithm for optimization

To improve model performance and avoid arbitrary hyperparameter selection, the sparrow search algorithm (SSA) was employed to optimize the key hyperparameters of the five ML models. SSA is a population-based swarm intelligence algorithm inspired by the foraging and anti-predation behavior of sparrows (Xue and Shen 2020). Owing to its simple structure, strong global search ability, and fast convergence, SSA has been widely used in parameter optimization problems.

In SSA, producers, scroungers, and sentinels jointly balance global exploration and local exploitation during iterative optimization. For producers, their positions are updated adaptively according to the current search state, which can be expressed as:

$$c_{i,j}^{a+1} = \begin{cases} c_{i,j}^{a} \cdot exp\left(-\frac{i}{\alpha \cdot \mathrm{iter}_{max}}\right), R < ST \\ c_{i,j}^{a} + Q \cdot L, R \geq ST \end{cases} \tag{2}$$

where $c_{i,j}^{a}$, $c_{i,j}^{a+1}$ denote the position of the i-th sparrow in the j-th dimension at the a-th and $(a+1)$-th iterations, respectively; iter_{max} is the maximum iterations; $\alpha \in (0,1]$; $R \in [0,1]$ is a warning threshold; $ST \in [0.5,1]$ is a safety threshold; Q follows a normal distribution; and $\mathbf{L}$ is a unit matrix.

The position of scroungers is updated according to the location of producers and the current global best/worst solutions, allowing the population to further exploit potentially optimal regions. Meanwhile, sentinels adjust their positions when danger is detected, thereby helping the swarm escape from local optima and improving the robustness of the search process.

In this study, SSA was used to optimize the principal hyperparameters of BPNN, XGBoost, SVM, ELM, and RF. For BPNN and ELM, the optimization mainly focused on the hidden-layer structure and other training-related parameters. For SVM, the penalty coefficient and kernel-related parameters were optimized. For XGBoost and RF, the optimization targeted the key tree-structure and ensemble-control parameters. The search ranges of all optimized hyperparameters were predefined based on commonly used values in previous studies and preliminary trial experiments, so as to ensure sufficient exploration while avoiding excessive computational cost. During the iterative search, parameter combinations with lower fitness values were progressively retained. The final search ranges and optimized values are summarized later in Table 5.

By introducing SSA-based optimization, the developed models became less dependent on empirical parameter selection, and the comparison among different algorithms was made more objective and reliable.

Model implementation and evaluation metrics

All models were implemented in MATLAB, and the overall prediction framework is illustrated in Fig. 4. The dataset was first divided into training and testing subsets; normalization parameters were calculated from the training set and then applied to both subsets according to the procedure described in Sect. "Data partitioning and normalization."

For each model, SSA was used to optimize the key hyperparameters before final training. In the optimization process, each sparrow represented one candidate hyperparameter combination, and the *RMSE* on the training set was used as the fitness value. After iterative optimization, the best hyperparameter combination was adopted to construct the final prediction model. The optimized hyperparameters and

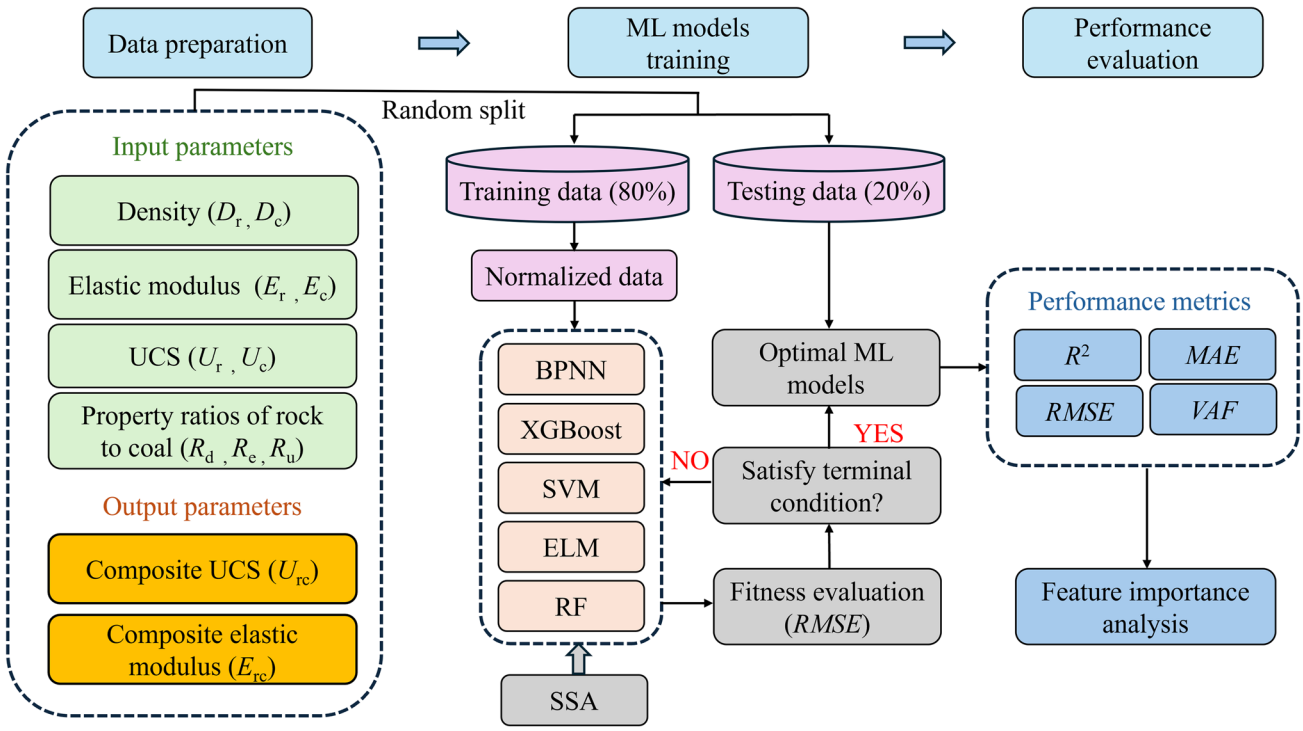

Fig. 4 Workflow of the ML model framework for predicting the mechanical parameters of coal–rock composites

Table 2 Performance metrics

Metrics	Expression	Ideal Value
R^2	$\frac{\sum_{i=1}^{n}(A_i-A_{avg})^2-\sum_{i=1}^{n}(A_i-P_i)^2}{\sum_{i=1}^{n}(A_i-A_{avg})^2}$	1
$RMSE$	$\sqrt{\frac{1}{n}\sum_{i=1}^{n}(A_i-P_i)^2}$	0
MAE	$\frac{1}{n}\sum_{i=1}^{n}\lvert P_i-A_i\rvert$	0
VAF	$\left(1-\frac{var(A_i-P_i)}{var(A_i)}\right)\times 100\%$	100

convergence behavior are discussed in Sect. "Model comparison and hyperparameter analysis."

Model performance was evaluated using four regression metrics: the coefficient of determination (R^2), $RMSE$, mean absolute error (MAE), and variance accounted for (VAF), with reference to established methodologies (Chai and Draxler 2014; Kumar et al. 2022, 2023a, 2023b; Kumar et al. 2024). Higher R^2 and VAF and lower $RMSE$ and MAE indicate better predictive performance. The definitions of these evaluation metrics are summarized in Table 2, where P_i and A_i denote the predicted and actual values of the i-th sample, respectively, and n is the total number of samples. Together, these metrics were used to compare the fitting accuracy, prediction error, and generalization performance of the five models.

Results and discussion

Model performance and comparative analysis

The predictive performance of the SSA-optimized machine learning models is summarized in Table 3 and Figs. 5, 6, 7 and 8. For U_{rc} prediction, SSA–SVM achieved the best overall test performance, with $R^2=0.90$ and $RMSE=3.98$, whereas SSA-ELM showed the lowest accuracy. SSA–XGBoost and SSA–RF also performed well, but their final prediction accuracy remained slightly lower than that of SSA-SVM.

The superior performance of SSA–SVM may be attributed to its kernel-based nonlinear mapping and strong generalization ability, which are particularly suitable for limited and heterogeneous datasets. In contrast, SSA–BPNN and SSA–ELM appeared more sensitive to initialization and data heterogeneity, likely reduced their predictive stability. The relatively good performance of SSA–XGBoost and SSA–RF further indicates that ensemble-based methods are effective in capturing nonlinear relationships in coal–rock composite data.

Table 3 Comparison of performance metrics of various ML models

ML models		Training dataset				Testing dataset			
		R^2	*VAF*	*MAE*	*RMSE*	R^2	*VAF*	*MAE*	*RMSE*
BPNN	U_{rc}	0.80	80.48	3.05	4.34	0.82	85.88	3.63	4.85
	E_{rc}	0.89	89.21	0.41	0.65	0.78	79.67	0.71	1.67
XGBoost	U_{rc}	0.91	91.49	1.71	3.02	0.86	86.29	2.49	3.48
	E_{rc}	0.66	66.75	0.75	1.25	0.77	77.23	0.52	0.67
SVM	U_{rc}	0.96	96.51	0.56	1.76	0.90	90.77	3.12	3.98
	E_{rc}	0.99	98.86	0.10	0.20	0.85	85.82	0.64	1.01
ELM	U_{rc}	0.74	73.59	3.64	5.21	0.77	77.52	3.80	4.77
	E_{rc}	0.77	77.22	0.66	0.96	0.76	76.03	0.84	1.06
RF	U_{rc}	0.93	92.87	1.90	2.81	0.90	90.38	1.94	2.61
	E_{rc}	0.63	62.96	0.65	1.17	0.71	71.53	0.80	1.30

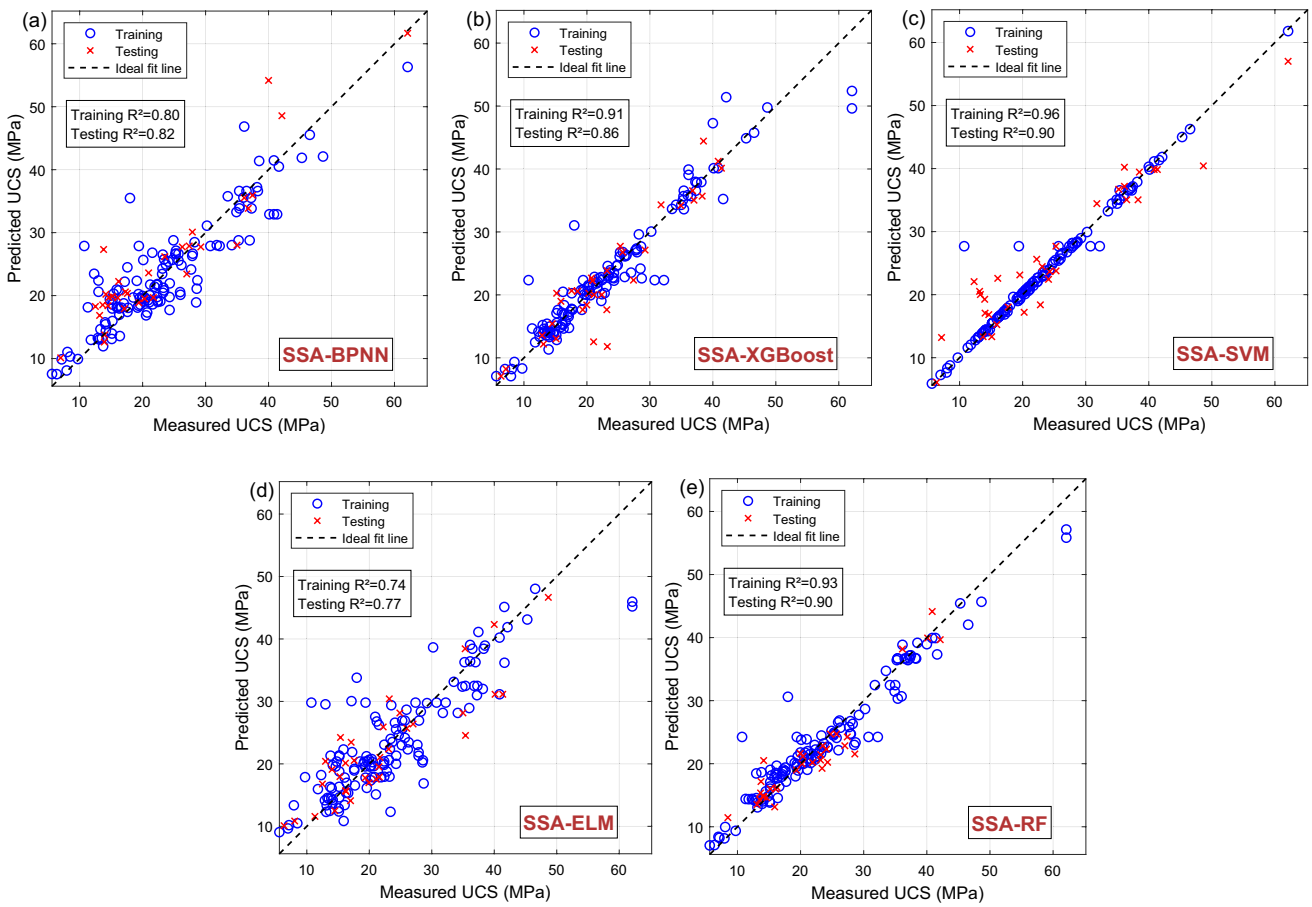

Fig. 5 Comparison between the measured and predicted UCS values for the training and testing datasets: **a** SSA–BPNN, **b** SSA–XGBoost, **c** SSA–SVM, **d** SSA–ELM, and **e** SSA–RF

For E_{rc} prediction, SSA–SVM again achieved the best performance ($R^2 = 0.85$), while SSA–RF showed lower accuracy ($R^2 = 0.71$) (as shown in Fig. 7). The moderate performance of BPNN suggests that increasing network complexity does not necessarily improve performance under limited-sample conditions. Instead, robust generalization appears to be more important than model complexity for the present dataset.

Another notable feature is the difference between training and testing performance. SSA–XGBoost achieved high training accuracy for U_{rc} prediction ($R^2 = 0.91$) but showed a moderate decline on the testing set ($R^2 = 0.86$),

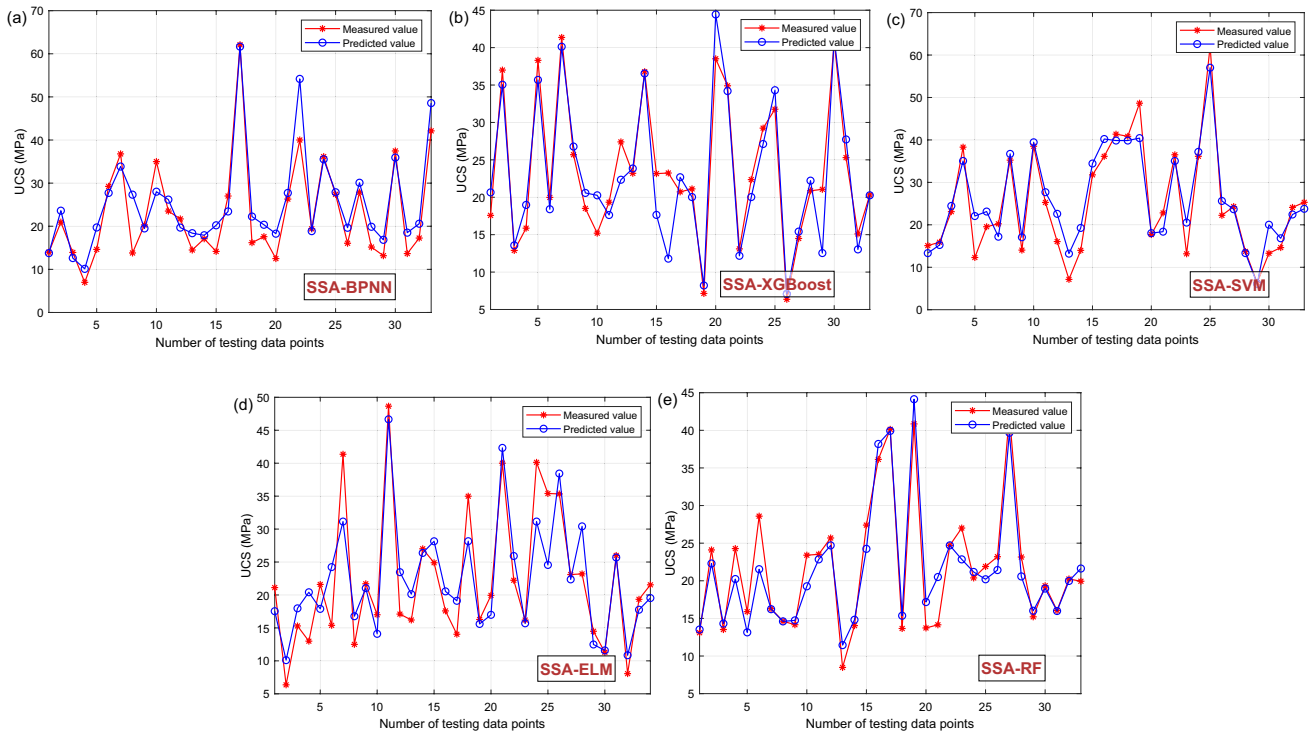

Fig. 6 UCS prediction performance of various models on the testing dataset: **a** SSA–BPNN, **b** SSA–XGBoost, **c** SSA–SVM, **d** SSA–ELM, **e** SSA–RF

indicating mild overfitting. SSA–ELM showed only a small decrease from training to testing, indicating acceptable generalization, although its absolute accuracy remained lower than that of SSA–SVM. By contrast, SSA–SVM maintained consistently strong performance on both the training and testing sets, demonstrating better generalization and more stable predictive behavior. Overall, these results suggest that model suitability for coal–rock composite prediction depends not only on nonlinear fitting ability, but also on the capacity to maintain robust generalization under limited and heterogeneous data conditions.

Feature importance analysis

The importance of input features was evaluated for the five ML models, as shown in Figs. 9 and 10. To improve interpretive rigor, the feature importance results were analyzed together with the Spearman correlation matrix in Fig. 3, so that the dominant features could be interpreted from both model-based rankings and their statistical associations with the target mechanical properties.

For U_{rc} prediction, the constituent strength parameters, especially coal strength (U_c), consistently ranked among the most influential variables across the models, as shown in Fig. 9. This is consistent with the correlation analysis, in which U_c showed a stronger positive association with U_{rc}, than rock strength (U_r) (as shown in Fig. 3). The result suggests that the composite strength is strongly controlled by the weaker constituent, in agreement with the weakest-link interpretation of coal–rock failure (Zuo et al. 2013). In addition, the rock-to-coal strength ratio (R_u) and coal proportion (R_c) were also identified as important factors. Their roles are also supported by the Spearman analysis, in which R_c and R_u show negative associations with U_{rc}. A higher R_c increases the proportion of the weaker coal phase and therefore reduces the overall composite strength, whereas a larger R_u reflects a stronger strength mismatch between rock and coal, which may intensify interfacial stress concentration and promote premature instability.

For E_{rc} prediction, coal proportion (R_c) was the most influential variable, followed by the constituent elastic moduli (E_c and E_r) and the rock-to-coal modulus ratio (R_e) (as shown in Fig. 10). This pattern is broadly consistent with the correlation matrix, in which E_{rc} is positively associated with the elastic properties of the constituent materials, while the influence of structural proportion and modulus mismatch is also evident. These results suggest that composite stiffness depends not only on the absolute stiffness of coal and rock, but also on their relative proportion and modulus mismatch, which together affect deformation compatibility and stress

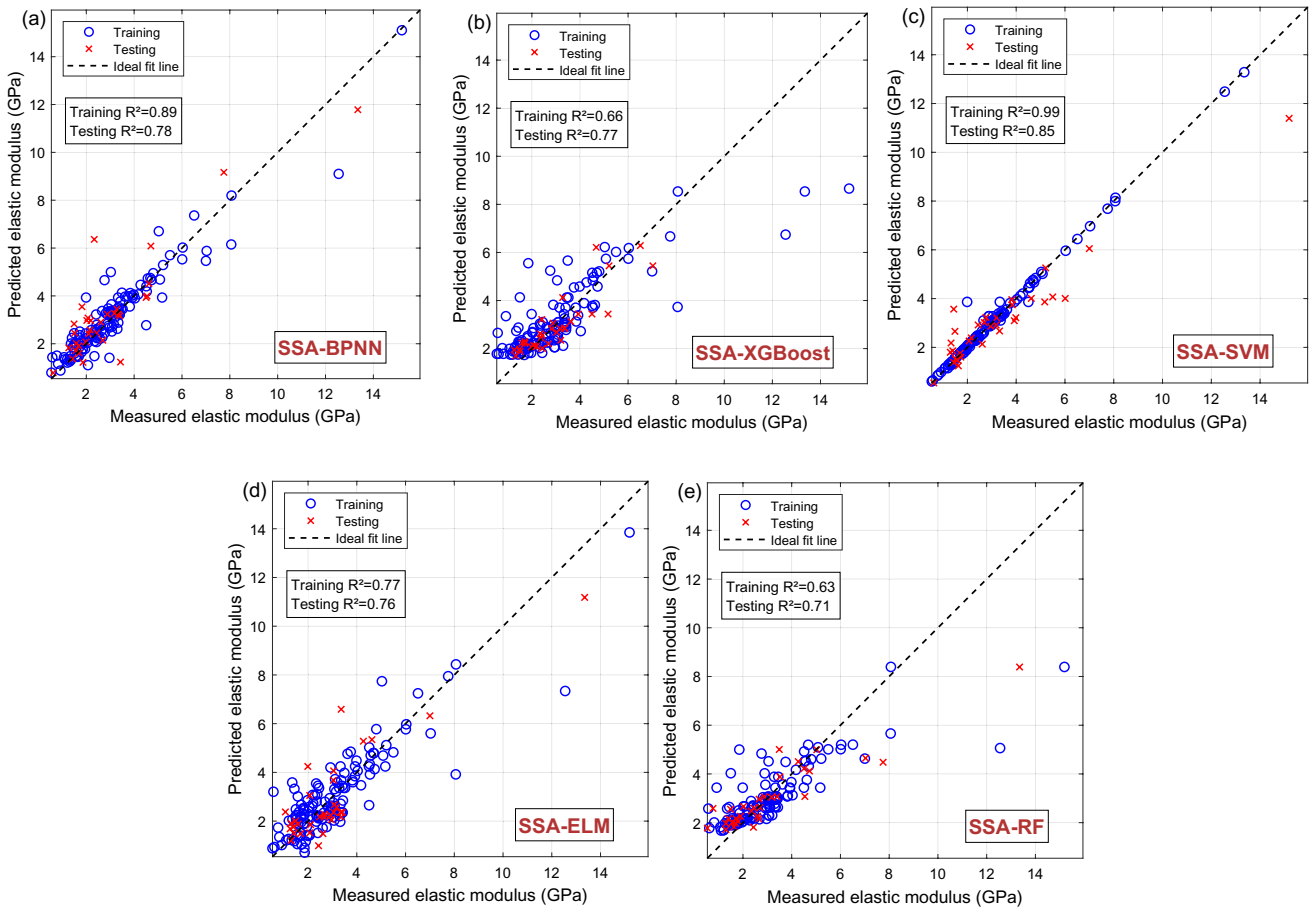

Fig. 7 Comparison between the measured and predicted elastic modulus values for the training and testing datasets: **a** SSA–BPNN, **b** SSA–XGBoost, **c** SSA–SVM, **d** SSA–ELM and **e** SSA–RF

redistribution within the composite (Chai et al. 2023; Chen et al. 2019; Wang et al. 2024).

The consistency between feature importance and correlation analysis reinforces the reliability of the interpretation. Variables that rank highly in the ML models, such as U_c, R_c, R_u, and R_e, also show meaningful statistical associations with U_{rc} or E_{rc} in the Spearman matrix. At the same time, differences between the two analyses are expected. Spearman correlation only describes pairwise monotonic association between two variables, whereas feature importance reflects the contribution of each variable within a multivariate nonlinear prediction framework. Therefore, a variable with moderate pairwise correlation may still receive high model importance if it contributes significantly through nonlinear interactions with other variables. Overall, the combined evidence indicates that coal–rock composite behavior is governed not by any single parameter alone, but by the coupled effects of constituent properties, material proportion, and mechanical mismatch (Hu et al. 2022; Tan et al. 2022).

Multi-parameter synergistic effects

The following discussion should be interpreted as a qualitative analysis of coupled parameter effects based on feature importance rankings, correlation trends, and mechanical reasoning, rather than as a fully quantitative interaction analysis. The feature importance results further reveal that the five ML models differed in how they captured the coupled effects of material proportion, strength contrast, and stiffness compatibility in coal–rock composites. These differences provide additional insight into why the models showed different predictive performance.

For SSA–SVM, the RBF kernel enhanced sensitivity to coal proportion (R_c) and the rock-to-coal strength ratio (R_u), indicating that this model was particularly effective in identifying nonlinear interactions associated with weak-phase dominance and strength mismatch. This is mechanically meaningful because R_c controls the relative contribution

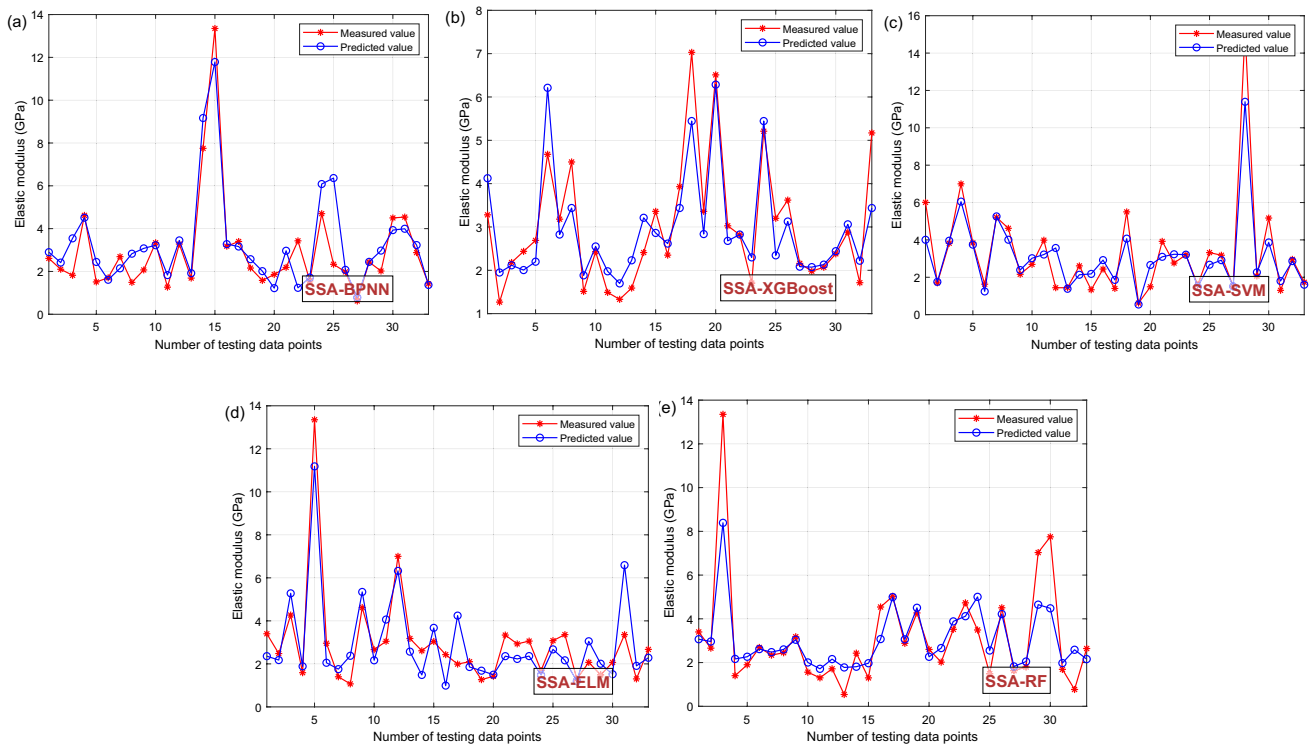

Fig. 8 Elastic modulus prediction performance of various models on the testing dataset: **a** SSA–BPNN, **b** SSA–XGBoost, **c** SSA–SVM, **d** SSA–ELM and **e** SSA–RF

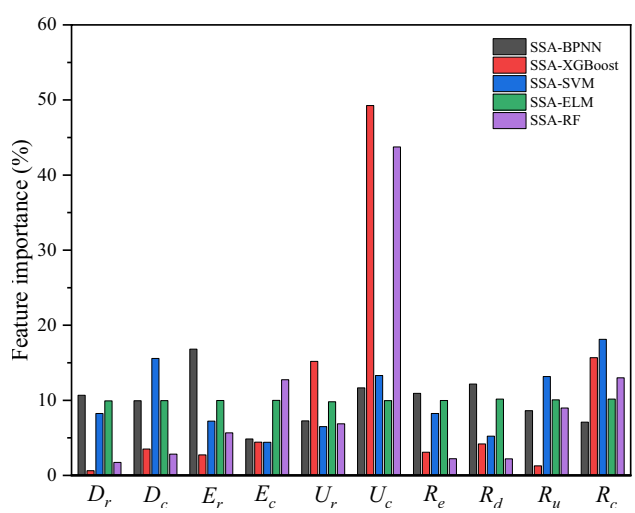

Fig. 9 Feature importance for composite UCS in different ML models

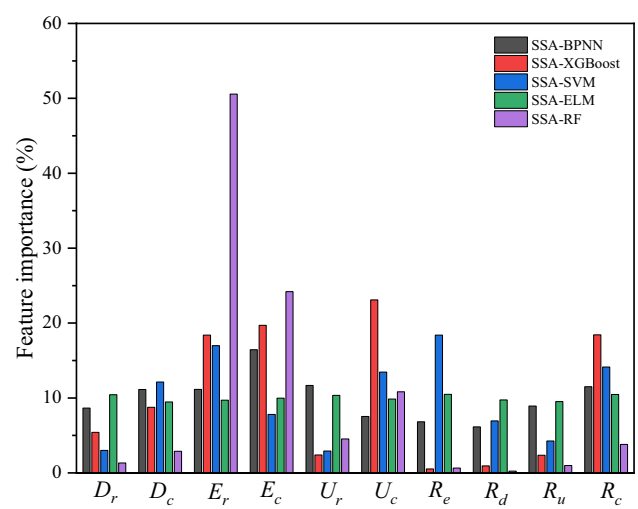

Fig. 10 Feature importance for composite elastic modulus in different ML models

of the weaker coal phase, whereas R_u reflects the degree of strength contrast between coal and rock, which affects load transfer and interfacial stress concentration. The strong sensitivity of SSA–SVM to these coupled variables helps explain its superior performance in the present dataset.

Neural-network-based models, especially SSA–BPNN and SSA–ELM, showed relatively greater sensitivity to density-related variables. Although density may reflect lithological differences that influence crack propagation and energy dissipation, these variables were not the most direct controls on composite strength and stiffness in the present dataset. In particular, the near-uniform feature importance distribution of SSA–ELM suggests limited

ability to distinguish dominant variables from secondary factors, which is consistent with its weaker predictive performance.

In contrast, the tree-based models SSA–RF and SSA–XGBoost were more sensitive to coal-related intrinsic properties, such as coal density, coal elastic modulus, and coal strength. This indicates that ensemble methods were effective in capturing heterogeneous local patterns associated with the coal component, but were relatively less effective than SSA–SVM in representing the broader coupled interactions among R_c, R_u, and stiffness mismatch.

Overall, coal–rock composite behavior cannot be interpreted from any single variable alone. The results suggest that material proportion, strength contrast, and stiffness compatibility may jointly affect the predicted mechanical response. A higher R_c generally weakens the composite, whereas larger strength or modulus mismatch may intensify interfacial incompatibility and promote premature instability. These observations provide qualitative data-driven evidence for coupled parameter effects, although more rigorous quantitative interaction analysis is still needed in future studies.

Model comparison and hyperparameter analysis

Advantages and limitations of each model

Table 4 summarizes the main strengths and limitations of the five ML models in terms of predictive ability, robustness, computational characteristics, and generalization performance in this study. As shown in Table 4, the comparative results indicate that model suitability for coal–rock composite prediction depends on both nonlinear fitting capacity and generalization robustness. SSA–SVM achieved the best overall performance, suggesting that kernel-based nonlinear mapping is particularly effective for limited and heterogeneous datasets. SSA–XGBoost and SSA–RF also showed good robustness, indicating that ensemble-based methods can effectively capture complex variable interactions. In contrast, SSA–BPNN and SSA-ELM were more sensitive to model structure and initialization, which may reduce stability when the available data are limited.

Table 5 Hyperparameter search ranges and optimized values obtained by SSA

Model	Hyperparameter	Search range	Optimized value
SVM	C (regularization parameter)	[0.1, 100]	10.1
	γ (RBF kernel parameter)	[0.001, 10]	2.3
XGBoost	*n_estimators*	[10, 200]	150
	max_depth	[1, 12]	5
	learning_rate	[0.01, 2]	0.39
RF	*n_estimators*	[50, 300]	100
	max_depth	[3, 15]	6
BPNN	Hidden layer 1 nodes	[5, 30]	15
	Hidden layer 2 nodes	[3, 15]	10
ELM	Hidden nodes	[10, 150]	30

Hyperparameter optimization analysis

The SSA algorithm was employed to optimize the key hyperparameters of each model. Table 5 presents the corresponding search ranges and optimized values. The search intervals were determined based on commonly used ranges reported in previous studies, preliminary trial experiments, and the trade-off between search breadth and computational cost. Excessively narrow intervals may miss promising solutions, whereas overly broad intervals may increase optimization difficulty and runtime.

As shown in Table 5, the optimized values for most models were located within the interior of the predefined search intervals rather than at the boundaries, indicating that the selected search spaces were generally appropriate. For example, the optimal C and γ values of SSA–SVM were 10.1 and 2.3, respectively, while SSA–XGBoost achieved its best performance at *n_estimators* =150, *max_depth* =5, and *learning_rate* =0.39.

Table 4 Comparative analysis of the advantages and limitations of different models

Model	Advantages	Limitations
SSA–BPNN	Captured nonlinear patterns effectively	More sensitive to network structure and initialization
SSA–XGBoost	Showed strong predictive ability and robustness	Involved more hyperparameters and a relatively more complex tuning process
SSA–SVM	Achieved the best overall prediction accuracy and generalization,	Performance remained highly dependent on the selection of C and γ
SSA–ELM	Offered fast training efficiency	Stability and feature discrimination ability were comparatively weaker
SSA–RF	Exhibited good robustness and resistance to overfitting	Final accuracy was slightly lower than that of the best-performing models

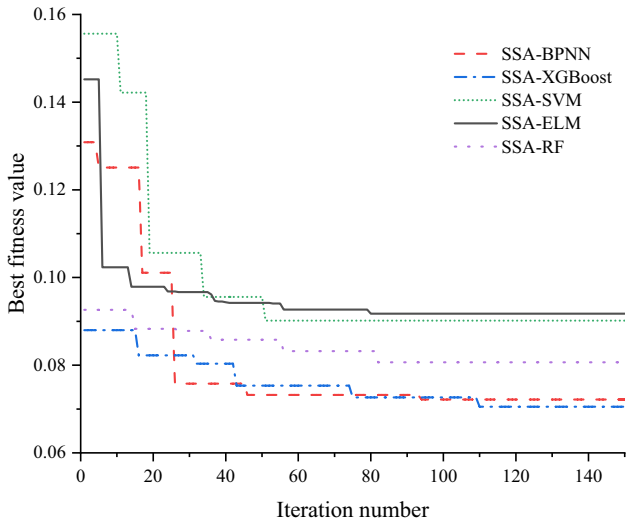

Fig. 11 Convergence curves of the best SSA fitness values for different ML models

Figure 11 shows the convergence curves of SSA for each model. The fitness values of all models decreased markedly during the first 20–50 iterations and then gradually approached stable levels. Most models converged before approximately 120 iterations, indicating that the maximum iteration number used in this study was sufficient to ensure convergence without obvious under-optimization. Since SSA is a stochastic optimization algorithm, the convergence curves in Fig. 11 represent the best fitness evolution from a representative optimization run for each model. Therefore, they mainly illustrate the convergence tendency and optimization behavior of SSA rather than the complete statistical variability across repeated independent runs.

Despite its effectiveness, SSA still has several limitations. Its performance depends on settings such as population size and iteration number, and larger populations increase computational cost. In addition, because SSA is stochastic, the optimization results may vary slightly across runs. As with other metaheuristic algorithms, SSA may also become trapped in local optima in highly complex search spaces.

The optimization results also provide insight into model applicability under limited-sample conditions. The superior performance of SSA–SVM after optimization suggests that, for the present dataset, robustness and generalization were more important than model complexity alone. By contrast, models with greater structural flexibility did not necessarily achieve better predictive performance, implying that overly parameterized architectures may be less advantageous for relatively limited and heterogeneous datasets.

Engineering implications and limitations

Although the dataset used in this study contains only 162 samples and remains limited for some lithological combinations, the proposed ML framework still has practical value for deep mining engineering. By using readily measurable properties of the constituent materials, such as uniaxial compressive strength, density, and elastic modulus, the framework enables preliminary estimation of the mechanical behavior of coal–rock composites without extensive preparation and testing of composite specimens. This is particularly useful when direct laboratory testing is impractical because of coal brittleness, coring costs, limited specimen availability, or time constraints during mine planning and design.

From an engineering perspective, the proposed framework is most suitable for preliminary assessment and screening rather than direct final design. It may support early-stage roadway support design, pillar stability evaluation, and hazard zoning by rapidly identifying lithological combinations associated with weak mechanical compatibility or elevated instability risk. The results also suggest that coal proportion and coal–rock strength mismatch should be explicitly considered when evaluating local support demand and failure susceptibility in heterogeneous mining environments.

Nevertheless, several limitations should be noted. The dataset remains relatively limited, and some lithological combinations are underrepresented, which may affect model generalizability. Although the selected variables are physically interpretable, potential redundancy may exist because the ratio-derived variables are mathematically related to the original coal and rock properties. Future studies should further examine feature robustness and interaction effects using ablation analysis, recursive feature elimination, and larger standardized datasets.

Conclusions

This study developed a data-driven framework for predicting the uniaxial compressive strength (U_{rc}) and elastic modulus (E_{rc}) of coal–rock composites using five SSA-optimized machine learning models, namely BPNN, XGBoost, SVM, ELM, and RF. Based on a compiled dataset of 162 samples, the predictive performance, feature importance, and engineering relevance of these models were systematically evaluated. Consequently, the study concludes that:

(a) Among the investigated models, SSA–SVM achieved the best overall predictive performance for both U_{rc} and E_{rc}, with testing R^2 values of 0.90 and 0.85,

respectively, indicating strong generalization ability under limited-sample conditions. In contrast, SSA-ELM and SSA–BPNN showed comparatively weaker performance, suggesting that neural-network-based approaches were more sensitive to dataset heterogeneity and feature discrimination limitations in the present problem.

(b) Feature importance analysis and correlation analysis consistently indicated that coal proportion (R_c) and the rock-to-coal strength ratio (R_u) are important variables associated with the predicted mechanical behavior of coal–rock composites. A higher R_c generally reduces the overall composite strength, while a larger strength contrast between rock and coal may intensify interfacial stress concentration and promote premature failure. These findings provide qualitative data-driven insights into the possible coupled effects of material proportion and mechanical mismatch.

(c) From an engineering perspective, the proposed framework can serve as a practical auxiliary tool for preliminary assessment in deep mining applications, such as roadway support design, pillar stability evaluation, and hazard screening. Nevertheless, its applicability remains constrained by dataset size, incomplete representation of interface and loading effects, and the need for further site-specific validation. Overall, the study demonstrates the potential of ML-based approaches for predicting coal–rock composite mechanical properties and provides a useful basis for future data-driven and mechanism-informed investigations.

Supplementary Information The online version contains supplementary material available at https://doi.org/10.1007/s11600-026-01946-w.

Acknowledgements This work was financially supported by the National Natural Science Foundation of China (grant No. 41972256) and the Fundamental Research Funds for the Central Universities (grant No. JZ2023HGTB0236). The sponsorship guaranteed with basic research funds provided by Politecnico di Torino, Italy for their financial aids in this work is also acknowledged. The authors also acknowledge the basic research funding provided by Politecnico di Torino, Italy.

Author contributions Qinghua Ou: writing—original draft, methodology, formal analysis, and conceptualization. Giuseppe Lacidogna: supervision, conceptualization, and writing—review and editing. Luwang Chen: supervision, investigation, funding acquisition, and writing—review and editing. Xiaowei Hou: funding acquisition, methodology. Xunjian Hu: methodology and software. Jiawei Song: data curation. All authors read and approved the final manuscript.

Funding Open access funding provided by Politecnico di Torino within the CRUI-CARE Agreement. This work was supported by the National Natural Science Foundation of China (Grant No. 41972256) and the Fundamental Research Funds for the Central Universities (Grant No. JZ2023HGTB0236).

Data availability The dataset used in this study was compiled from 47 published experimental studies. The processed dataset supporting the findings of this work is provided in Online Appendix A. The original data sources are listed in the reference section and Online Appendix A for traceability.

Declarations

Conflict of interest The authors declare that they have no known competing financial interests or personal relationships that could have appeared to influence the work reported in this paper.

Open Access This article is licensed under a Creative Commons Attribution 4.0 International License, which permits use, sharing, adaptation, distribution and reproduction in any medium or format, as long as you give appropriate credit to the original author(s) and the source, provide a link to the Creative Commons licence, and indicate if changes were made. The images or other third party material in this article are included in the article's Creative Commons licence, unless indicated otherwise in a credit line to the material. If material is not included in the article's Creative Commons licence and your intended use is not permitted by statutory regulation or exceeds the permitted use, you will need to obtain permission directly from the copyright holder. To view a copy of this licence, visit http://creativecommons.org/licenses/by/4.0/.

References

Aboutaleb S, Behnia M, Bagherpour R, Bluekian B (2017) Using non-destructive tests for estimating uniaxial compressive strength and static Young's modulus of carbonate rocks via some modeling techniques. Bull Eng Geol Environ 77(4):1717–1728. https://doi.org/10.1007/s10064-017-1043-2

ASTM International (2023) Standard test method for compressive strength and elastic moduli of intact rock core specimens under varying states of stress and temperatures. ASTM International, West Conshohocken, PA

Barzegar R, Sattarpour M, Deo R, Fijani E, Adamowski J (2019) An ensemble tree-based machine learning model for predicting the uniaxial compressive strength of travertine rocks. Neural Comput Appl 32(13):9065–9080. https://doi.org/10.1007/s00521-019-04418-z

Breiman L (2001) Random forests. Mach Learn 45:5–32. https://doi.org/10.1023/A:1010933404324

Ceryan N (2014) Application of support vector machines and relevance vector machines in predicting uniaxial compressive strength of volcanic rocks. J Afr Earth Sci 100:634–644. https://doi.org/10.1016/j.jafrearsci.2014.08.006

Chai T, Draxler RR (2014) Root mean square error (RMSE) or mean absolute error (MAE)? – arguments against avoiding RMSE in the literature. Geosci Model Dev 7(3):1247–1250. https://doi.org/10.5194/gmd-7-1247-2014

Chai Y, Dou L, Cai W, Małkowski P, Li X, Gong S, Bai J, Cao J (2023) Experimental investigation into damage and failure process of coal-rock composite structures with different roof lithologies under mining-induced stress loading. Int J Rock Mech Min Sci. https://doi.org/10.1016/j.ijrmms.2023.105479

Chen S, Ge Y, Yin D, Yang H, Sarhosis V (2019) An experimental study of the uniaxial failure behaviour of rock-coal composite samples with pre-existing cracks in the coal. Adv Civ Eng. https://doi.org/10.1155/2019/8397598

Chen L, Ou Q, Peng Z, Wang Y, Chen Y, Tian Y (2022) Numerical simulation of abnormal roof water-inrush mechanism in mining under unconsolidated aquifer based on overburden dynamic

damage. Eng Fail Anal. https://doi.org/10.1016/j.engfailanal.2021.106005

Chen T, Guestrin C (2016) XGBoost: A scalable tree boosting system, In: Proceedings of the 22nd ACM SIGKDD international conference on knowledge discovery and data mining, pp. 785–794.

Dehghan S, Sattari G, Chehreh Chelgani S, Aliabadi MA (2010) Prediction of uniaxial compressive strength and modulus of elasticity for Travertine samples using regression and artificial neural networks. Min Sci Technol 20(1):41–46. https://doi.org/10.1016/s1674-5264(09)60158-7

Drucker H, Burges CJ, Kaufman L, Smola A, Vapnik V (1996) Support vector regression machines. Adv Neural Inf Process Syst 9

Fathipour-Azar H (2021) Machine learning-assisted distinct element model calibration: ANFIS, SVM, GPR, and MARS approaches. Acta Geotech 17(4):1207–1217. https://doi.org/10.1007/s11440-021-01303-9

Fu Y, He Y, Li C, Yin D (2023) Failure and acoustic emissions of coal–rock combinations with different dip angles in the Shaqu No. 1 coal mine. Adv Civ Eng 2023:1–17. https://doi.org/10.1155/2023/9969802

Gao H, Zhai Y, Wang T, Li Y, Meng F, Zhang H, Li Y (2023) Compression failure conditions of concrete-granite combined body with different roughness interface. Int J Min Sci Technol 33(3):297–307. https://doi.org/10.1016/j.ijmst.2022.12.002

Guo W, Hu Y, Wu D (2023) Simulation experimental investigations into the mechanical response and failure mechanisms of coal–rock combinations. Sustainability. https://doi.org/10.3390/su152015175

Han S, Li H, Li M, Rose T (2019) A deep learning based method for the non-destructive measuring of rock strength through hammering sound. Appl Sci. https://doi.org/10.3390/app9173484

He M, Wang Q, Wu Q (2021) Innovation and future of mining rock mechanics. J Rock Mech Geotech Eng 13(1):1–21. https://doi.org/10.1016/j.jrmge.2020.11.005

He M, Cheng T, Qiao Y, Li H (2023) A review of rockburst: experiments, theories, and simulations. J Rock Mech Geotech Eng 15(5):1312–1353. https://doi.org/10.1016/j.jrmge.2022.07.014

Hoek E, Brown ET (2019) The Hoek–Brown failure criterion and GSI – 2018 edition. J Rock Mech Geotech Eng 11(3):445–463. https://doi.org/10.1016/j.jrmge.2018.08.001

Hu J, Li J, Ma D (2022) Effect of loading rates on mechanical characteristics and rock burst tendency of coal-rock combined samples. Adv Mater Sci Eng 2022:1–10. https://doi.org/10.1155/2022/8176721

Hu X, Shentu J, Xie N, Huang Y, Lei G, Hu H, Guo P, Gong X (2023) Predicting triaxial compressive strength of high-temperature treated rock using machine learning techniques. J Rock Mech Geotech Eng 15(8):2072–2082. https://doi.org/10.1016/j.jrmge.2022.10.014

Huang B, Liu J (2013) The effect of loading rate on the behavior of samples composed of coal and rock. Int J Rock Mech Min Sci 61:23–30. https://doi.org/10.1016/j.ijrmms.2013.02.002

Huang G-B, Zhu Q-Y, Siew C-K (2006) Extreme learning machine: theory and applications. Neurocomputing 70(1):489–501. https://doi.org/10.1016/j.neucom.2005.12.126

Huang S, He Y, Yu S, Cai C (2022) Experimental investigation and prediction model for UCS loss of unsaturated sandstones under freeze-thaw action. Int J Min Sci Technol 32(1):41–49. https://doi.org/10.1016/j.ijmst.2021.10.012

Indraratna B, Armaghani DJ, Gomes Correia A, Hunt H, Ngo T (2023) Prediction of resilient modulus of ballast under cyclic loading using machine learning techniques. Transp Geotech. https://doi.org/10.1016/j.trgeo.2022.100895

Jiang Z, Zhu Z, Accornero F (2024a) Tensile-to-shear crack transition in the compression failure of steel-fibre-reinforced concrete: insights from acoustic emission monitoring. Buildings 14(7):2039. https://doi.org/10.3390/buildings14072039

Jiang Z, Zhu Z, Accornero F, Wang C (2024b) Multi-technique analysis of seawater impact on the performance of calcium sulphoaluminate cement mortar. Constr Build Mater 443:137717. https://doi.org/10.1016/j.conbuildmat.2024.137717

Jing G, Zhao Y, Gao Y, Marin Montanari P, Lacidogna G (2023) Noise reduction based on improved variational mode decomposition for acoustic emission signal of coal failure. Appl Sci 13:9140. https://doi.org/10.3390/app13169140

Jing G, Zhao Y, Wang H, Montanari PM, Lacidogna G (2024) Study of coal and magnetite collapse process and precursor based on acoustic emission flicker noise spectroscopy. Rock Mech Rock Eng 57(10):8545–8562. https://doi.org/10.1007/s00603-024-03989-1

Jing G, Lacidogna G, Zhao Y, Marin Montanari P, Rojo Tanzi BN, Iturrioz I (2025) Coal–rock catastrophic collapse: precursors based on AE and fiber bundle models. Int J Geomech 25(1):04024314. https://doi.org/10.1061/IJGNAI.GMENG-9857

Jitchaijaroen W, Keawsawasvong S, Wipulanusat W, Kumar DR, Jamsawang P, Sunkpho J (2024) Machine learning approaches for stability prediction of rectangular tunnels in natural clays based on MLP and RBF neural networks. Intell Syst Appl. https://doi.org/10.1016/j.iswa.2024.200329

Jodeiri Shokri B, Mirzaghorbanali A, McDougall K, Karunasena W, Nourizadeh H, Entezam S, Hosseini S, Aziz N (2024) Data-driven optimised XGBoost for predicting the performance of axial load bearing capacity of fully cementitious grouted rock bolting systems. Appl Sci. https://doi.org/10.3390/app14219925

Kakasor Ismael Jaf D, Ismael Abdulrahman P, Salih Mohammed A, Kurda R, Qaidi SMA, Asteris PG (2023) Machine learning techniques and multi-scale models to evaluate the impact of silicon dioxide (SiO2) and calcium oxide (CaO) in fly ash on the compressive strength of green concrete. Constr Build Mater. https://doi.org/10.1016/j.conbuildmat.2023.132604

Khatti J, Grover KS (2024) Assessment of the uniaxial compressive strength of intact rocks: an extended comparison between machine and advanced machine learning models. Multiscale Multidiscip Model Exp des 7(4):3301–3325. https://doi.org/10.1007/s41939-024-00408-4

Kumar DR, Samui P, Burman A (2022) Determination of best criteria for evaluation of liquefaction potential of soil. Transp Infrastruct Geotechnol 10(6):1345–1364. https://doi.org/10.1007/s40515-022-00268-w

Kumar DR, Samui P, Wipulanusat W, Keawsawasvong S, Sangjinda K, Jitchaijaroen W (2023a) Soft-computing techniques for predicting seismic bearing capacity of strip footings in slopes. Buildings. https://doi.org/10.3390/buildings13061371

Kumar R, Kumar A, Ranjan Kumar D (2023b) Buckling response of CNT based hybrid FG plates using finite element method and machine learning method. Compos Struct 319:117204. https://doi.org/10.1016/j.compstruct.2023.117204

Kumar M, Samui P, Armaghani DJ (2024) A novel approach to estimate rock deformation under uniaxial compression using a machine learning technique. Bull Eng Geol Environ. https://doi.org/10.1007/s10064-024-03775-x

Lai X, Xu H, Shan P, Hu Q, Ding W, Yang S, Yan Z (2024) Research on the mechanism of rockburst induced by mined coal-rock linkage of sharply inclined coal seams. Int J Miner Metall Mater 31(5):929–942. https://doi.org/10.1007/s12613-024-2833-8

Li W, Bai J, Cheng J, Peng S, Liu H (2015) Determination of coal–rock interface strength by laboratory direct shear tests under constant normal load. Int J Rock Mech Min Sci 77:60–67. https://doi.org/10.1016/j.ijrmms.2015.03.033

Li X, Chen S, Wang E, Li Z (2021) Rockburst mechanism in coal rock with structural surface and the microseismic (MS) and

electromagnetic radiation (EMR) response. Eng Fail Anal. https://doi.org/10.1016/j.engfailanal.2021.105396

Li C, Zhou J, Dias D, Du K, Khandelwal M (2023) Comparative evaluation of empirical approaches and artificial intelligence techniques for predicting uniaxial compressive strength of rock. Geosciences (Basel). https://doi.org/10.3390/geosciences13100294

Liu XS, Tan YL, Ning JG, Lu YW, Gu QH (2018) Mechanical properties and damage constitutive model of coal in coal-rock combined body. Int J Rock Mech Min Sci 110:140–150. https://doi.org/10.1016/j.ijrmms.2018.07.020

Ngo TQ, Nguyen LQ, Tran VQ (2023) Novel hybrid machine learning models including support vector machine with meta-heuristic algorithms in predicting unconfined compressive strength of organic soils stabilised with cement and lime. Int J Pavemen Eng 24(2):2136374. https://doi.org/10.1080/10298436.2022.2136374

Niu Y, Wang E, Li Z, Gao F, Zhang Z, Li B, Zhang X (2022) Identification of coal and gas outburst-hazardous zones by electric potential inversion during mining process in deep coal seam. Rock Mech Rock Eng 55(6):3439–3450. https://doi.org/10.1007/s00603-022-02804-z

Paudel S, Pudasaini A, Shrestha RK, Kharel E (2023) Compressive strength of concrete material using machine learning techniques. Cleaner Eng Technol. https://doi.org/10.1016/j.clet.2023.100661

Qiao Z, Li C, Wang Q, Xu X (2024) Principles of formulating measures regarding preventing coal and gas outbursts in deep mining: Based on stress distribution and failure characteristics. Fuel. https://doi.org/10.1016/j.fuel.2023.129578

Qiu L, Song D, He X, Wang E, Li Z, Yin S, Wei M, Liu Y (2020) Multifractal of electromagnetic waveform and spectrum about coal rock samples subjected to uniaxial compression. Fractals. https://doi.org/10.1142/s0218348x20500619

Qiu D, Li X, Xue Y, Fu K, Zhang W, Shao T, Fu Y (2023) Analysis and prediction of rockburst intensity using improved D-S evidence theory based on multiple machine learning algorithms. Tunnelling Underground Space Technol. https://doi.org/10.1016/j.tust.2023.105331

Rajabi M, Beheshtian S, Davoodi S, Ghorbani H, Mohamadian N, Radwan AE, Alvar MA (2021) Novel hybrid machine learning optimizer algorithms to prediction of fracture density by petrophysical data. J Pet Explor Prod Technol 11(12):4375–4397. https://doi.org/10.1007/s13202-021-01321-z

Rumelhart D, Hinton G, Williams R (1986) Learning representations by back-propagating errors. Nature 323:533–536

Shaunik D, Singh M (2019) Strength behaviour of a model rock intersected by non-persistent joint. J Rock Mech Geotech Eng 11(6):1243–1255. https://doi.org/10.1016/j.jrmge.2019.01.004

Shen W, Yu W, Pan B, Li K (2022) Rock mechanical failure characteristics and energy evolution analysis of coal-rock combination with different dip angles. Arab J Geosci. https://doi.org/10.1007/s12517-021-09268-5

Tan Y, Ma Q, Liu X, Zhao Z, Zhao M, Li L (2022) Failure prediction from crack evolution and acoustic emission characteristics of coal-rock sandwich composite samples under uniaxial compression. Bull Eng Geol Environ. https://doi.org/10.1007/s10064-022-02705-z

Tian M, Zhang A, Yin D, Xiao H, Han L, Liu Z (2024) Research on mechanical characteristics and failure mechanism of coal-rock combined bodies with equal strength. KSCE J Civ Eng 28(10):4678–4691. https://doi.org/10.1007/s12205-024-2637-4

Tran DT, Onjaipurn T, Kumar DR, Chim-Oye W, Keawsawasvong S, Jamsawang P (2024) An eXtreme gradient boosting prediction of uplift capacity factors for 3D rectangular anchors in natural clays. Earth Sci Inform 17(3):2027–2041. https://doi.org/10.1007/s12145-024-01269-8

Ulusay R, Hudson J (eds) (2007) The complete ISRM suggested methods for rock characterization, testing and monitoring: 1974-2006. International Society for Rock Mechanics (ISRM), Berlin, Germany

Wang Q, Wang J, Ye Y, Jiang W, Yao N (2020a) Failure characteristics and strength model of composite rock samples in contact zone under compression. Arch Min Sci 65(2):347–361. https://doi.org/10.24425/ams.2020.133197

Wang T, Ma Z, Gong P, Li N, Cheng S, Yin Z (2020b) Analysis of failure characteristics and strength criterion of coal-rock combined body with different height ratios. Adv Civ Eng. https://doi.org/10.1155/2020/8842206

Wang W, Wang H, Zhang B, Wang S, Xing W (2021) Coal and gas outburst prediction model based on extension theory and its application. Process Saf Environ Prot 154:329–337. https://doi.org/10.1016/j.psep.2021.08.023

Wang M, Zhao G, Liang W, Wang N (2023a) A comparative study on the development of hybrid SSA-RF and PSO-RF models for predicting the uniaxial compressive strength of rocks. Case Stud Constr Mater. https://doi.org/10.1016/j.cscm.2023.e02191

Wang Y, Hasanipanah M, Rashid ASA, Le BN, Ulrikh DV (2023b) Advanced tree-based techniques for predicting unconfined compressive strength of rock material employing non-destructive and petrographic tests. Materials (Basel). https://doi.org/10.3390/ma16103731

Wang W, Wang K, Zhang X, Jiang Y, Cai T, Yan J, Yue S (2024) Mechanical properties of coal-rock combined bodies under the action of ScCO2: A study of damage and failure mechanism. Eng Fail Anal. https://doi.org/10.1016/j.engfailanal.2023.107807

Wang C, Jiang Z, Accornero F, Zhou S, Ou Q (2025) Influence of seawater and salt ions on the properties of calcium sulfoaluminate cement. J Mater Civil Eng. https://doi.org/10.1061/jmcee7.Mteng-19193

Xie Z, Zhang N, Meng F, Han C, An Y, Zhu R (2019) Deformation field evolution and failure mechanisms of coal–rock combination based on the digital speckle correlation method. Energies. https://doi.org/10.3390/en12132511

Xu D, Wang Y, Huang J, Liu S, Xu S, Zhou K (2023) Prediction of geology condition for slurry pressure balanced shield tunnel with super-large diameter by machine learning algorithms. Tunnelling Underground Space Technol. https://doi.org/10.1016/j.tust.2022.104852

Xu C, Wang W, Wang K, Hu K, Cao Z, Zhang Y (2024a) Influence of coal-rock interface inclination on the damage and failure law of original coal-rock combination. Eng Fail Anal. https://doi.org/10.1016/j.engfailanal.2024.108275

Xu C, Yang T, Wang K, Yuan Y, Guo L (2024b) Influence of primary interface characteristics on mechanical properties and damage evolution of coal-rock combination. Eng Fail Anal. https://doi.org/10.1016/j.engfailanal.2024.108658

Xue J, Shen B (2020) A novel swarm intelligence optimization approach: sparrow search algorithm. Syst Sci Control Eng 8(1):22–34. https://doi.org/10.1080/21642583.2019.1708830

Yang L, Gao F, Wang X (2020) Mechanical response and energy partition evolution of coal-rock combinations with different strength ratios. Chin J Rock Mech Eng. https://doi.org/10.13722/j.cnki.jrme.2020.0456

Yilmaz I, Yuksek G (2009) Prediction of the strength and elasticity modulus of gypsum using multiple regression, ANN, and ANFIS models. Int J Rock Mech Min Sci 46(4):803–810. https://doi.org/10.1016/j.ijrmms.2008.09.002

Yin D, Chen S, Sun X, Jiang N (2023) Strength characteristics of roof rock-coal composite samples with different height ratios under uniaxial loading. Arch Min Sci. https://doi.org/10.24425/ams.2019.128685

Yu W, Wu G, Pan B, Wu Q, Liao Z (2021) Experimental investigation of the mechanical properties of sandstone–coal–bolt specimens with different angles under conventional triaxial compression. Int J Geomech. https://doi.org/10.1061/(asce)gm.1943-5622.0002005

Zhang H, Wu S, Zhang Z (2022) Prediction of uniaxial compressive strength of rock via genetic algorithm—selective ensemble learning. Nat Resour Res 31(3):1721–1737. https://doi.org/10.1007/s11053-022-10065-4

Zhao Z-h, Wang W-m, Dai C-q, Yan J-x (2014) Failure characteristics of three-body model composed of rock and coal with different strength and stiffness. Trans Nonferrous Met Soc China 24(5):1538–1546. https://doi.org/10.1016/s1003-6326(14)63223-4

Zhao C, Cao S, Lang S, Du S, Che C (2024) Uniaxial compressive failure characteristics and fractal analysis of mud–sand composite rock samples based on acoustic emission tests. Fractal Fract. https://doi.org/10.3390/fractalfract8120713

Zhu Z, Jiang Z, Accornero F, Carpinteri A (2024) Correlation between seismic activity and acoustic emission on the basis of in situ monitoring. Nat Hazards Earth Syst Sci 24(11):4133–4143. https://doi.org/10.5194/nhess-24-4133-2024

Zuo J, Wang Z, Zhou H, Pei J, Liu J (2013) Failure behavior of a rock-coal-rock combined body with a weak coal interlayer. Int J Min Sci Technol 23(6):907–912. https://doi.org/10.1016/j.ijmst.2013.11.005

Publisher's Note Springer Nature remains neutral with regard to jurisdictional claims in published maps and institutional affiliations.